

Grant Agreement No.:

Project acronym: GaSTech

Project title: Demonstration of Gas Switching Technology for Accelerated Scale-up of Pressurized Chemical Looping Applications

Funding scheme

Thematic Priority:

THEME:

Starting date of project: 1st of August, 2017

Duration: 36 months

| WP N° | Del. N° | Title | Contributors | Lead beneficiary | Nature | Dissemination level | Delivery date from Annex I | Actual delivery date dd/mm/yyyy |
|-------|---------|--------------------------------------|--|------------------|--------|---------------------|----------------------------|------------------------------------|
| 3 | 3.1 | Initial gas switching reactor models | Jan Hendrik Cloete (NTNU), Schalk Cloete (SINTEF) | SINTEF | R | PU | 31/01/2018 | 31/01/2018 |

1 Summary

This report details the development of OD reactor models for the four gas switching concepts investigated in the GaSTech project. The model assumes the reactor to be a continuously stirred tank reactor (CSTR) in thermal and chemical equilibrium, which is generally a good assumption in large fluidized bed reactors. Significant work was invested to automate the model to achieve targeted operating guidelines such as maximum temperature and degree of oxygen carrier utilization.

The model formulation is summarized in this report and simulation results are presented. Model outputs clearly illustrate the behaviour of the different gas switching technologies. In particular, guidelines for optimization are specified for each concept as follows:

- Gas switching combustion (GSC): Optimize the cycle time to balance CO₂ avoidance and outlet stream temperature.
 - Longer cycle time → Less mixing between CO₂ and N₂ → Better CO₂ avoidance
 - Shorter cycle time → Less temperature variation across the cycle → Higher average outlet temperature → Higher efficiency in the power cycle
 - Advanced heat management through N₂ dilution can maximize outlet temperature when long cycles are used
- Gas switching reforming (GSR): Optimize the cycle time to balance CO₂ avoidance and reactor temperature.
 - Longer cycle time → Less mixing between CO₂ and N₂ → Better CO₂ avoidance
 - Shorter cycle time → Less temperature variation across the cycle → Lower maximum reactor temperature → Cheaper reactor, outlet valves and filters
 - Additional thermal mass in the reactor can minimize temperature variations when longer cycles are used
- Gas switching water splitting (GSWS): Optimize reactor temperature to balance fuel conversion and hydrogen production.
 - Higher reactor temperature → More fuel conversion → Lower amount of process complexity to minimize fuel slip
 - Lower reactor temperature → Higher H₂ concentration in the water splitting stage → Lower steam requirement
 - A two-stage fuel stage may be necessary to minimize fuel slip
 - GSWS could also be operated for syngas production and, like GSR, be integrated with a PSA unit for pure hydrogen production
- Gas switching oxygen production (GSOP): Optimize reactor temperature to balance O₂ production and required air flow rate.
 - Higher reactor temperature → Higher concentration of O₂ in N₂-free outlet stream
 - Lower reactor temperature → More O₂ extraction from incoming air stream → Smaller depleted air stream that must be efficiently integrated in the process
 - The cycle time can be maximized to maximize O₂ separation efficiency as long as the oxygen carrier oxidation enthalpy is low enough

These insights combined with the optimized OD reactor model will streamline the screening of different process configurations over the next year of the project.

2 Summary of reactor concepts

Basic reactor behaviour of the four gas switching reactor concepts is summarized in Figure 1.

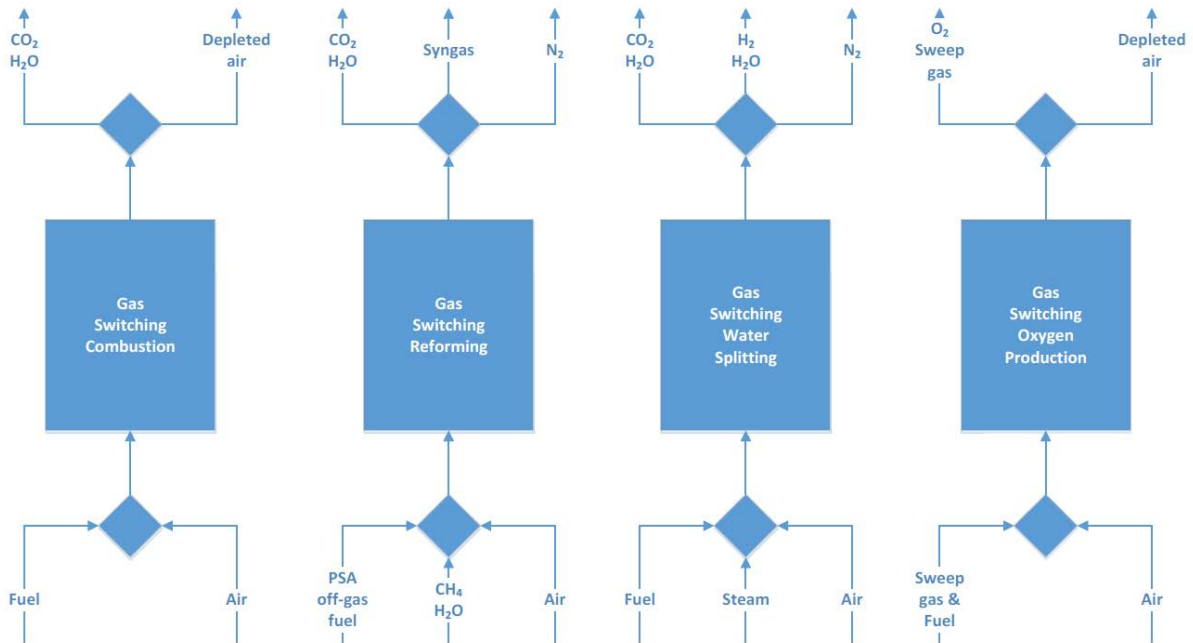


Figure 1: Illustration of reactor behaviour of the four reactor concepts investigated in the GaSTech project.

GSC simply cycles fuel and air to reduce and oxidize an oxygen carrier material. This allows fuel combustion with an inherently separated CO_2 stream exiting in the fuel stage.

GSR employs the same principle as GSC to combust a fuel gas. In this case, however, the heat of fuel combustion is not used to drive a power cycle, but rather to enable the endothermic steam-methane reforming reaction. The GSR concept thus requires an oxygen carrier that also serves as a catalyst for the reforming reaction. Integration into a hydrogen production process can allow for efficient use of the off-gas fuel from the pressure swing adsorption (PSA) unit in the fuel stage of the GSR reactors.

GSWS again follows the basic GSC principle to combust a fuel with inherent CO_2 separation. In this case, however, hydrogen is produced through water splitting, thus requiring specialized oxygen carriers that support this reaction. The advantage of GSWS over GSR is that no downstream process units are required to produce pure hydrogen. On the other hand, GSWS typically has a higher steam requirement than GSR and faces challenges with fuel slip.

GSOP is another variation on the GSC principle. In this case, a specialized oxygen carrier with the ability to release free oxygen is used. The oxygen carried by the oxygen carrier from the air stage to the fuel stage is thus not used to combust a fuel, but rather to produce an oxygen containing stream without any nitrogen. This stream can then be used to achieve oxyfuel CO_2 capture in downstream process units. A small quantity of fuel must also be fed to the fuel stage to maintain the reactor temperature.

3 Reactor simulations

All gas switching reactors were modelled as continuously stirred tank reactors (CSTR), which is generally a good assumption for a well-mixed fluidized bed. In addition, thermal and chemical equilibrium was assumed. Thermal equilibrium is easily achieved in fluidized beds due to the very fast gas-particle heat transfer resulting from the dynamic mixing and small particle size. Chemical equilibrium is also generally a good assumption in large fluidized beds where the gas residence time is large, giving ample time for reaction. As an example, a recent experimental demonstration of the GSR concept [1] showed that chemical equilibrium is reached even in a small lab-scale reactor where the gas residence time would be much shorter than in an industrial scale reactor.

3.1 Mole and energy balances

The following mole and energy balances are solved using the ode15 differential-algebraic equation solver in Matlab.

$$\frac{dN_{g,i}}{dt} = F_g^{in} y_{g,i}^{in} - F_g y_{g,i} + \sum_k s_{i,k} R_k \quad \text{Eq. 1}$$

$$\frac{dN_{s,j}}{dt} = \sum_k s_{j,k} R_k \quad \text{Eq. 2}$$

$$\left(\sum_i N_{g,i} C_{P,i} + \sum_j N_{s,j} C_{P,j} \right) \frac{dT}{dt} = \sum_i (F_g^{in} y_{g,i}^{in} h_{g,i}^{in} - F_g y_{g,i} h_{g,i}) + \sum_k R_k \Delta H_k^R \quad \text{Eq. 3}$$

In the gas species mole balance (Eq. 1), $N_{g,i}$ [kmol] is the gas holdup of gas species i . F_g^{in} and F_g [kmol/s] are the total molar flowrates into and out of the reactor respectively. The final term is the source term due to the different reactions, where $s_{i,k}$ is the stoichiometric constant of species i in reaction k , and R_k [kmol/s] is the rate of reaction k . The solids mole balance (Eq. 2) is similar for each species j , but there is no inflow or outflow of solids material in the gas switching reactors.

Eq. 3 shows the energy balance, where $C_{P,i}$ and $C_{P,j}$ [J/kmol.K] are the heat capacities of gas species i and solids species j respectively. T [K] is the temperature, while $h_{g,i}^{in}$ and $h_{g,i}$ [J/kmol] are the enthalpies of incoming and outgoing gas species i . All heat capacities and enthalpies are calculated as a function of temperature based on gas species data from Stull and Prophet [2] and solids species data from Robie and Hemingway [3]. ΔH_k^R [J/kmol] is the reaction enthalpy of reaction k at a reference temperature of 298 K.

Finally, the ideal gas law is used to specify the number of gas moles in the reactor.

$$PV_g = \sum_i N_i R_0 T \quad \text{Eq. 4}$$

Here, P [Pa] is the pressure, V_g [m³] is the gas volume (difference between reactor volume and solids volume), and R_0 [J/kmol.K] is the universal gas constant.

3.2 Reaction descriptions

Each gas switching concept involves a distinct set of reactions between the gas and the oxygen carrier particles. In general, reactions are implemented as illustrated for the hypothetical example below:



The example in Eq. 5 illustrates a heterogeneous equilibrium reaction where gas species A and solids species B react to form gas species C and solids species D (or vice versa). The general reaction rate expression for this reaction is given below:

$$R = \frac{1}{\tau} \left(p_A - \frac{p_C}{K} \right) N_{s,react} \quad \text{Eq. 6}$$

Here, τ is a reaction timescale that is set to a low value (e.g. 0.001) to ensure a very fast reaction so that chemical equilibrium is always achieved. K is the reaction equilibrium constant, p [bar] is the partial pressure of the gas species and $N_{s,react}$ [kmol] is the number of moles of solid reactant. In this case, the solid reactant would be species B if the reaction proceeds from left to right, and species D if the reaction proceeds from right to left. This ensures that the reaction stops when no solid reactant is present.

3.2.1 GSC reactions

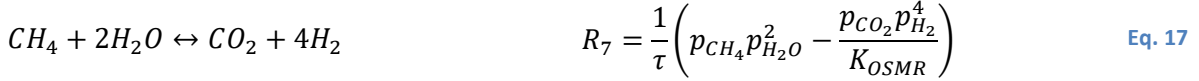
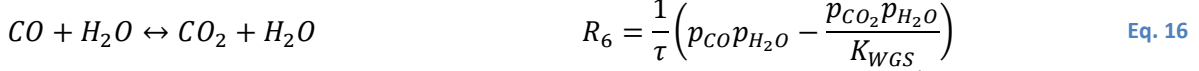
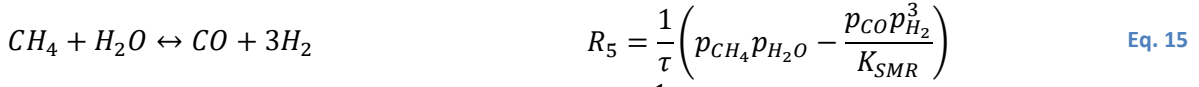
Ilmenite ore is considered as oxygen carrier in the GSC process. In this case, results from literature [4] suggest that the redox reactions can be approximated through four heterogeneous reactions. Eq. 7 - Eq. 9 take place primarily in the reduction step (fuel stage), whereas Eq. 10 mainly takes place in the oxidation step (air stage). All of the reactions in the GSC process will proceed until one of the reactants is consumed.



3.2.2 GSR reactions

Four heterogeneous and three catalytic reactions are simulated in this process. Eq. 11 - Eq. 13 mainly take place in the reduction step, Eq. 14 in the oxidation step, and Eq. 15 - Eq. 17 in the reforming step.





As is evident from the equations, Eq. 11 - Eq. 14 are assumed to proceed until one of the reactants is consumed, while Eq. 15 - Eq. 17 proceed to the equilibrium conditions proposed by Xu and Froment [5] (Eq. 18 - Eq. 20).

$$K_{SMR} = 1.2 \times 10^{13} \exp\left(\frac{-223080}{RT}\right) \quad \text{Eq. 18}$$

$$K_{WGS} = 0.0177 \exp\left(\frac{36580}{RT}\right) \quad \text{Eq. 19}$$

$$K_{OSMR} = 2.124 \times 10^{11} \exp\left(\frac{-168000}{RT}\right) \quad \text{Eq. 20}$$

3.2.3 GSWS reactions

In the water splitting process, iron oxide is used as oxygen carrier. In contrast to the GSC process, magnetite (Fe_3O_4) is considered as an intermediate step due to the important equilibrium reactions (Eq. 25 - Eq. 26) taking place when it is reduced to FeO . Eq. 21 - Eq. 26 primarily take place in the reduction step (fuel stage). The reverse reaction in Eq. 25 allows hydrogen to be produced in the water splitting stage when steam is fed to the reactor. In the air stage, primarily the reaction in Eq. 28 will occur, since the process is controlled to oxidise all FeO to Fe_3O_4 by the end of the water splitting stage.



In Eq. 25 - Eq. 26, N_{gas} is the total number of moles in the gas phase and $N_{s,react}$ is the number of moles of the solids species that are reacting, i.e., Fe_3O_4 in case of the forwards reaction and FeO in

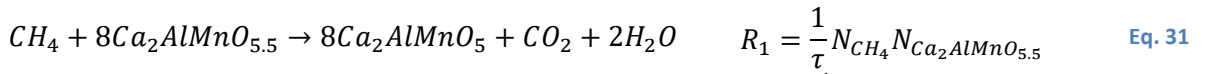
case of the backwards reaction. The equilibrium mole fractions are obtained by fitting curves to experimental results in literature [6].

$$\frac{y_{H_2,eq}}{y_{H_2,eq} + y_{H_2O}} = 1.847 \times 10^{-6} T^2 - 5.181 \times 10^{-3} T + 3.798 \quad \text{Eq. 29}$$

$$\frac{y_{CO,eq}}{y_{CO,eq} + y_{CO_2}} = 5.163 \times 10^{-7} T^2 - 1.517 \times 10^{-3} T + 1.376 \quad \text{Eq. 30}$$

3.2.4 GSOP reactions

The reduction reactions (Eq. 31 - Eq. 33) taking place primarily in the fuel stage in the GSOP process are similar to those in the GSC process, except for the different oxygen carrier that is used. The primary difference appears in the oxidation reaction (Eq. 34) where an oxygen carrier is utilised that will also release oxygen in the fuel stage.



In Eq. 34, the equilibrium mole fraction of O_2 , $y_{O_2,eq}$, has been determined in a previous study [7] as the following:

$$y_{O_2,eq} = \frac{1}{P} \exp\left(\frac{-91000}{R_0} \left(\frac{1}{T} - \frac{1}{873.15}\right)\right) \quad \text{Eq. 35}$$

Here, the pressure, P , is expressed in *bar*.

4 Results and discussion

Reactor simulation results for the four gas switching concepts are presented sequentially below. In each case, typical reactor behaviour will be illustrated, followed by a brief illustration of the optimization criteria of each individual concept.

4.1 GSC

Figure 2 shows the typical behaviour of the GSC process over an entire cycle. In the fuel stage (first 480 s), the oxygen carrier is reduced by the fuel, producing carbon dioxide and steam. During this stage, the reactor cools down due to slightly endothermic reactions and the relatively cold fuel gases entering the reactor.

In the subsequent air stage, the oxygen carrier is oxidised by air and heated by the highly exothermic reaction. In this example, air diluted with nitrogen is fed to the reactor. A previous study [8] has found that this practice can improve the overall plant efficiency by increasing the average reactor temperature. Nitrogen dilution limits the temperature rise due to the highly exothermic oxidation

reaction, since less oxygen is available to react with the oxygen carrier. This leads to less temperature variation during a cycle, leading to a higher average temperature when the maximum temperature during the cycle is fixed. However, this strategy comes at the cost of additionally plant complexity, since the depleted air from the outlet during the air stage needs to be recycled to use as feed gas.

Finally, the species profiles in Figure 2 show that nitrogen and CO₂ are kept separate in the different stages. However, a small amount of mixing occurs when switching between the stages due to the excellent mixing in fluidized bed reactors. This mixing is an inherent drawback of the fluidized bed gas switching principle and must be minimized.

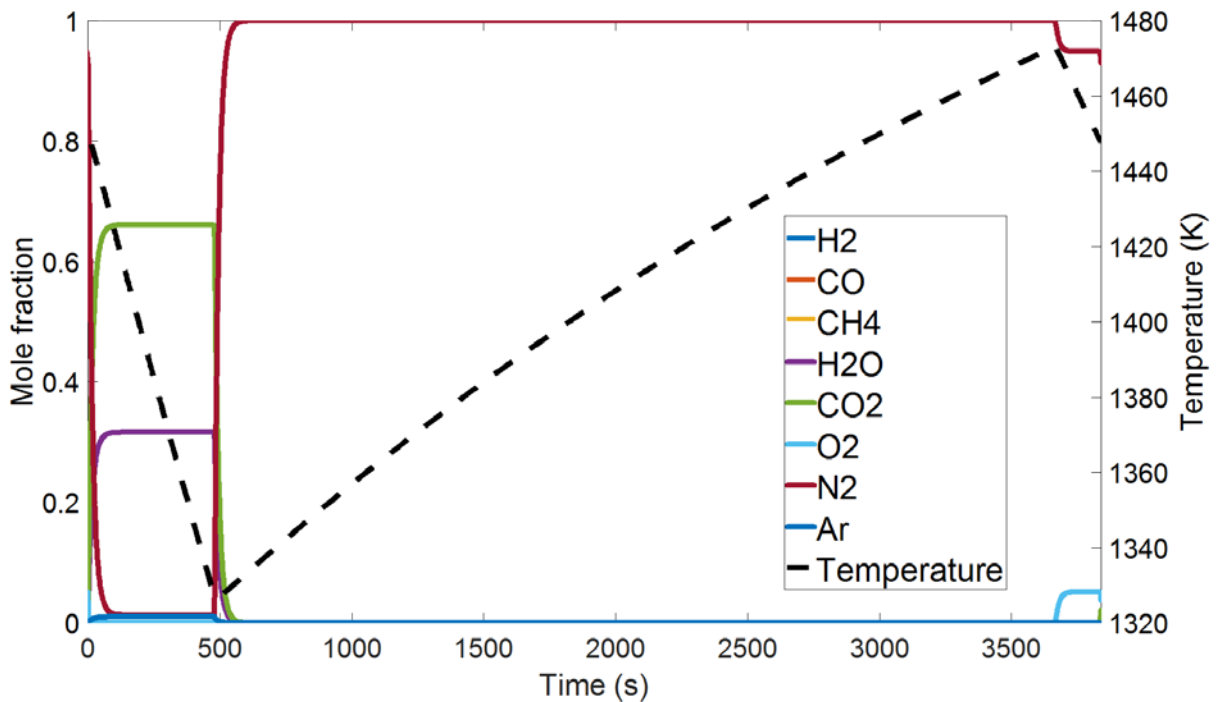


Figure 2: Reactor outlet gas species and temperature plot over one complete GSC cycle. In the first 480 s the oxygen carrier is reduced by fuel, whereas for the remainder of the process the oxygen carrier is oxidised by a depleted air stream.

The length of the stages (proportional to the percentage oxygen carrier utilization) is an important optimization parameter in the GSC process. On the one hand, by increasing the stage time, the relative amount of mixing when switching between the air and fuel stages is reduced, leading to a higher CO₂ capture efficiency and purity. On the other hand, increasing the stage times also increases the temperature variation over the cycle. The maximum allowable temperature in the cycle is limited by several components such as the reactor body, the oxygen carrier and the downstream switching valves and filters. For a fixed maximum reactor temperature, a larger temperature variation over the cycle leads to a lower average reactor temperature. An earlier study [8] showed that the overall efficiency of a power plant containing a GSC reactor cluster is reduced significantly as the average temperature of the outlet gases is decreased. The effects of changing the stage times on the overall plant performance are illustrated in Figure 3.

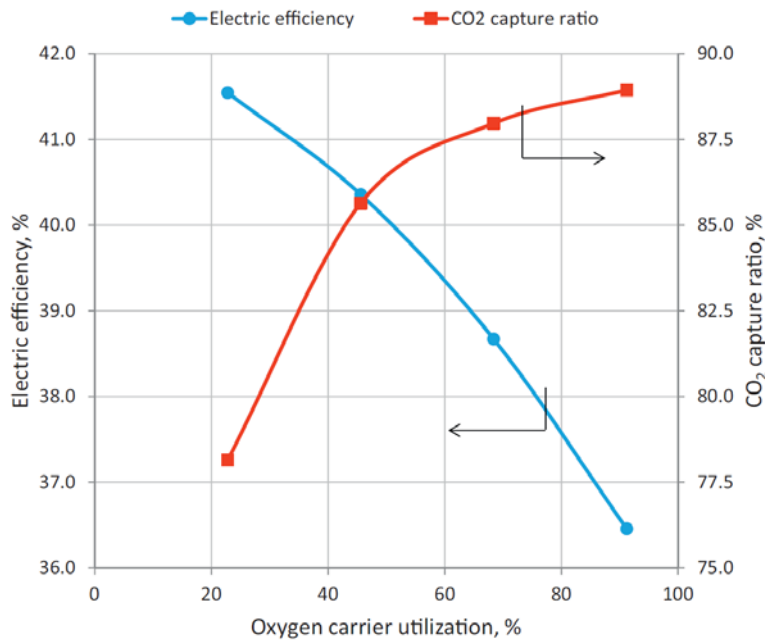


Figure 3: Power plant performance in terms of electric efficiency and CO₂ capture ratio for the different oxygen carrier utilization cases (proportional to the stage time) [8].

4.2 GSR

The basic behaviour of the GSR reactor is illustrated in Figure 4. During the reduction stage (first 300 s), all the incoming fuel gases are converted to CO₂ and H₂O and the reactor temperature slowly reduces, mostly due to the necessity to heat up the incoming fuel gases.

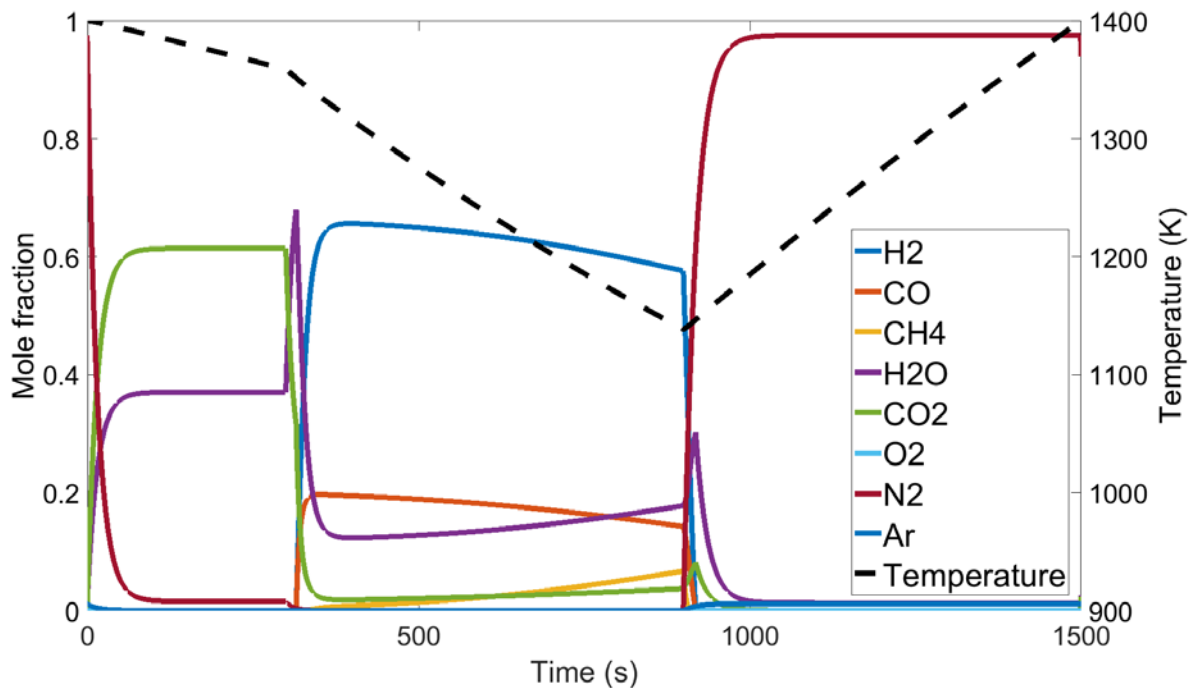


Figure 4: Reactor outlet gas species and temperature plot over one complete GSR cycle. The first 300 s of the cycle is reduction with PSA off-gas fuel, followed by 600 s of steam-methane reforming and 600 s of oxidation with air.

At the start of the reforming stage (300 s in Figure 4), some remaining NiO must still be reduced and the incoming CH₄ is therefore converted to H₂O and CO₂. Some NiO is purposefully left at the end of the reduction step to account for the fact that the reduction reaction rates will slow down as the oxygen carrier comes close to full conversion, potentially leading to some undesired fuel slip. After this brief initial period of complete oxygen carrier reduction, the reforming reactions take place, producing H₂ and CO. Due to the endothermic nature of the reforming reaction, the temperature drops faster than in the reduction stage. As the reactor temperature reduces, the CH₄ conversion and H₂ production also decline due to less favourable thermodynamics.

Finally, the oxidation stage starts (900 s in Figure 4) to oxidize the oxygen carrier and heat up the reactor. During the first few seconds of oxidation, some H₂ and CO left in the reactor are converted to H₂O and CO₂. Following this brief period, the outlet gases comprise of almost pure N₂ as all the O₂ in the air is consumed by the oxidation reaction.

Figure 4 also illustrates the undesired mixing between N₂ and CO₂ before and after the oxidation stage. Similar to the GSC case, the impact of this undesired mixing can be reduced by making the cycle time longer. Longer cycle times will reduce the length of the initial period of mixing relative to the subsequent period of pure gas production.

As in GSC, the trade-off linked to longer cycle times is more temperature variation across the cycle. In the case of GSR, a large temperature variation will cause a larger drop in temperature during the reforming stage, thus lowering the degree of methane conversion. A certain level of methane conversion is required for the process to operate correctly, implying that the average reforming stage temperature must be maintained at a certain level. The net effect of longer cycle times is therefore the necessity for a higher peak reactor temperature to maintain the necessary reforming temperature. The trade-off between CO₂ separation efficiency and maximum reactor temperature is illustrated in Figure 5 (left).

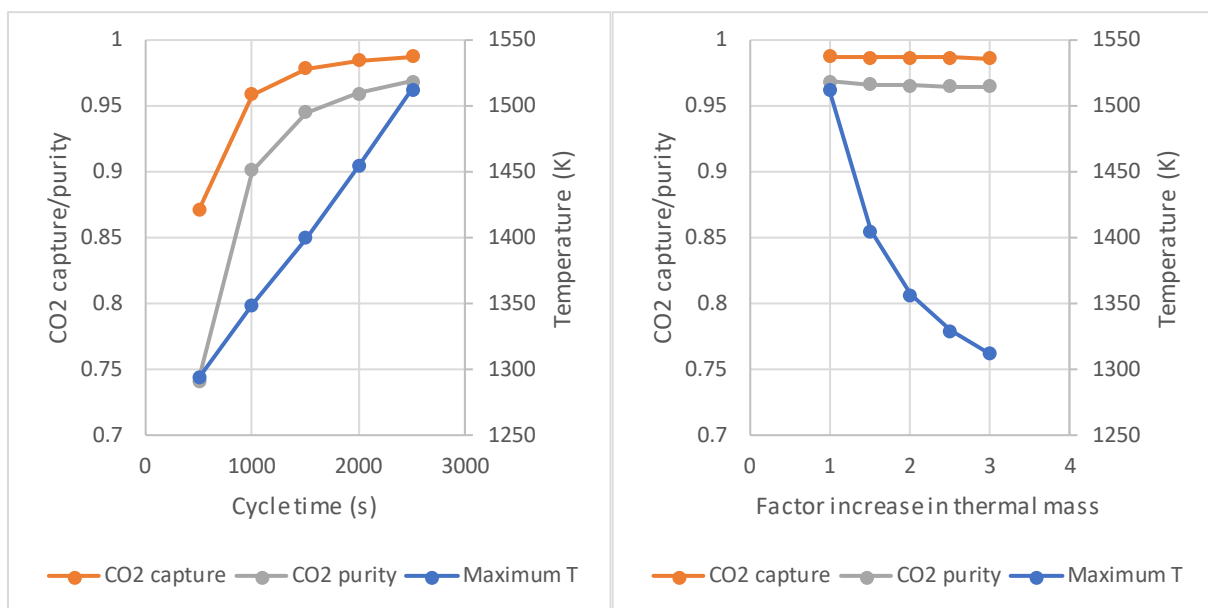


Figure 5: The effect of an increase in cycle time (left) and an increase in reactor thermal mass (right) on CO₂ separation efficiency and maximum reactor temperature. The graph on the right is carried out with 2500 s cycle time.

As discussed in the GSC case, the reactor and oxygen carrier as well as the downstream switching valves and filters must be designed for the maximum reactor temperature. A very high maximum reactor temperature can therefore significantly increase reactor costs and can even create insurmountable technical challenges. It is therefore desired that the maximum reactor temperature can be limited while still maintaining long cycle times.

This could potentially be achieved by adding additional thermal mass to the reactor (such as vertical metal rods) to slow down the temperature variation across the cycle. Figure 5 (right) illustrates the effect of including additional thermal mass for the longest cycle time studied (2500 s). The results show that additional thermal mass that will triple the thermal mass of the oxygen carrier (factor of 3 increase) will reduce the maximum reactor temperature by 200 K, significantly reducing costs and technical challenges related to very high temperature operating conditions.

4.3 GSWS

The typical behaviour of the GSWS process is shown in Figure 6 over one cycle. During the fuel stage (first 400 s), the oxygen carrier is reduced by fuel (methane) being fed to the reactor. In the first part of the fuel stage, hematite (Fe_2O_3) is converted to magnetite (Fe_3O_4) and the fuel is completely converted to steam and CO_2 . However, once the hematite is completely depleted, the equilibrium reactions from magnetite to wüstite (FeO), result in fuel slip in the form of carbon monoxide and hydrogen. The reactor temperature falls during the entire reduction stage, but the temperature drops faster during the second part where methane is essentially reformed to syngas in a more endothermic reaction.

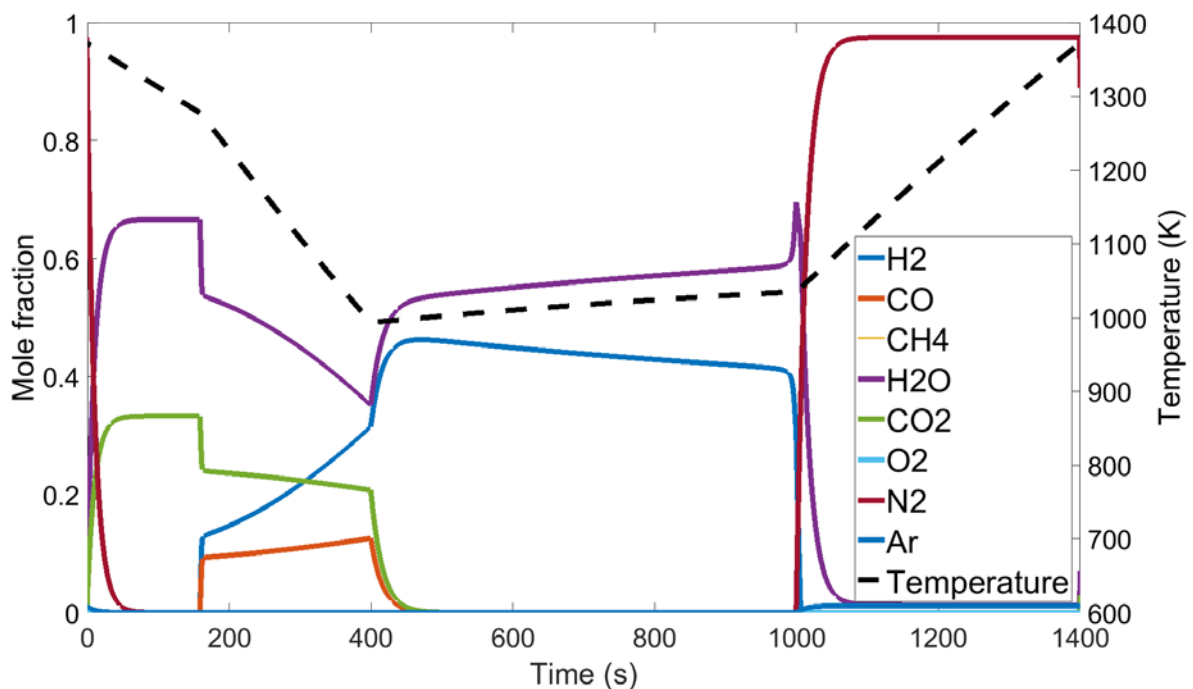


Figure 6: Species and temperature profiles over a typical GSWS cycle.

In the water splitting stage (400 s to 1 000s), steam is fed to the reactor. In the same equilibrium reaction as in the fuel stage, the steam then oxidizes the wüstite to magnetite, producing hydrogen.

During this stage, the slightly exothermic oxidation reaction and the requirement that the gases should be heated to the reactor temperature approximately balances, resulting in a relatively small temperature change.

In the final air stage, the oxygen carrier is completely oxidised to hematite by oxygen in air. The highly exothermic oxidation reaction also serves to heat up the reactor, allowing autothermal operation. As in GSC and GSR, the GSWS process inherently separates carbon dioxide in the fuel stage from nitrogen in the air stage, but a limited amount of undesired mixing occurs when switching between stages.

The reactor temperature has a strong influence on the equilibrium behaviour of the GSWS process. Specifically, higher temperatures promote the conversion of incoming fuel gases, while lower temperatures promote water splitting to produce hydrogen. This tradeoff was investigated by carrying out reactor simulations at different maximum reactor temperatures as shown in Figure 7. All simulations were carried out at the maximum possible cycle time because longer cycle times capitalize on the equilibrium behaviour of the GSWS process: the fuel stage takes place at higher temperatures where fuel conversion is better and water splitting takes place at lower temperatures where more hydrogen is produced (see Figure 6).

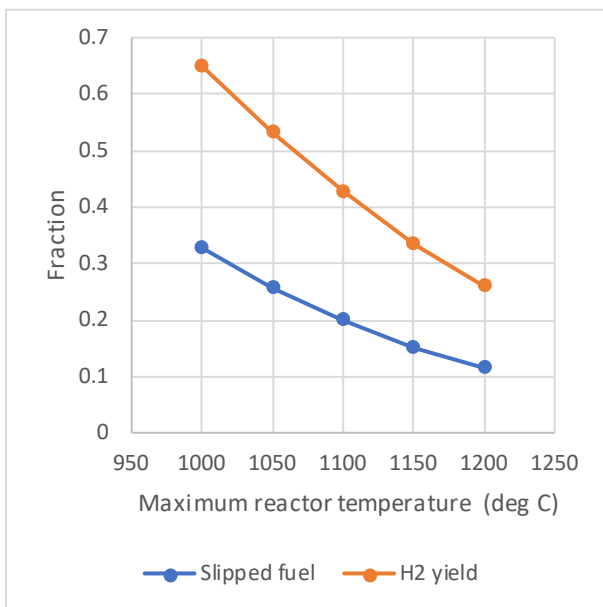


Figure 7: The fuel slip (fraction of unconverted fuel) and hydrogen production (fraction of hydrogen in water splitting stage outlet stream) as a function of maximum reactor temperature.

The effect of reactor equilibrium behaviour can clearly be observed in Figure 7. Higher temperatures achieve greater fuel conversion, but produce a lower hydrogen fraction during the water splitting stage. It should be noted, however, that the high hydrogen yields thermodynamically achievable at low temperatures may not be practically achievable because of kinetic limitations in the water splitting stage that takes place at low temperatures (typically about 350 °C lower than the maximum reactor temperature). Experimental tests in WP1 and WP2 will shed further light on this aspect.

In future work with process design, the efficient utilization of slipped fuel will be an important priority. If a large amount of slipped fuel can be accommodated in the process, the reactor can be operated at

lower temperatures, thus increasing the hydrogen yield. One potential use of the slipped fuel is to split the reduction stage into two. The slipped fuel from the second stage can then be fed to the first stage where it is completely converted by the hematite that is in the system at the start of reduction.

It is also interesting to note that the GSWS process essentially reforms methane to syngas in the second part of the reduction stage where maganetite is converted to wüstite. As such, the GSWS process can be operated very similarly to the GSR concept if the water splitting stage is simply omitted. The produced syngas in the second part of the reduction stage can then be fed to a PSA unit, with the PSA off-gas fuel being fed back to the first part of the reduction stage where hematite facilitates complete fuel conversion. This can be an interesting alternative in the event that GSWS oxygen carriers turn out to be significantly cheaper than GSR oxygen carriers (which require catalytic properties).

4.4 GSOP

The behaviour of the GSOP reactor is illustrated in Figure 8. In the reduction stage (first 600 s) a sweep gas stream (CO_2 and H_2O) with some added fuel (H_2 , CO and CH_4) is fed to the reactor. This gas stream reduces the local oxygen partial pressure, triggering the specialized GSWS oxygen carrier to release free oxygen. The limited amount of fuel gases is combusted by some of the released oxygen, thus increasing the reactor temperature, which triggers the release of more free oxygen by increasing the equilibrium oxygen partial pressure. The oxygen-rich stream from this stage can be used for downstream oxyfuel CO_2 capture purposes. As one example, it can be fed to a gasifier to increase the overall efficiency of the power plant, as discussed in an earlier study [7].

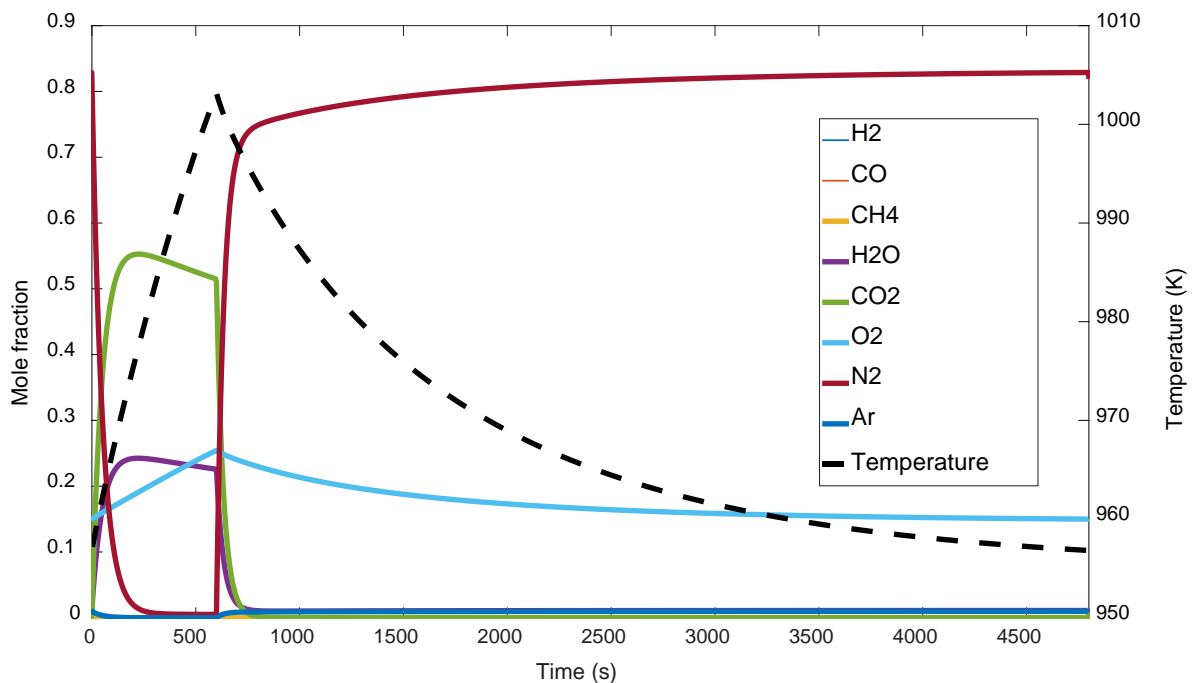


Figure 8: Reactor outlet gas species and temperature plot over one complete GSOP cycle.

During the longer air stage that follows, the oxygen carrier is oxidised with air and the reactor is cooled down again. Even though the oxidation reaction is also exothermic, the reactor temperature drops because only a small percentage of the oxygen in the incoming air reacts before equilibrium is reached.

The moderately heated air stream exiting the air stage of the GSOP process presents the most important process integration challenge with this concept. This stream is generally quite large and must be further heated up before useful work can be generated at a high efficiency. It is therefore desirable to keep this stream as small as possible to minimize this process integration challenge.

As mentioned earlier, the equilibrium oxygen mole fraction in the reactor increases with increasing reactor temperature. An increase in temperature can be achieved by increasing the amount of fuel gases in the sweep stage. In this way, more of the oxygen released in the reduction stage will combust the fuel instead of exiting the reactor unreacted, thus generating more heat. Such an increase in reactor temperature will increase the percentage of oxygen in the N_2 -free outlet stream from the reduction stage, but it will also increase the magnitude of the semi-hot depleted air stream exiting the oxidation stage. This trade-off is illustrated in Figure 9.

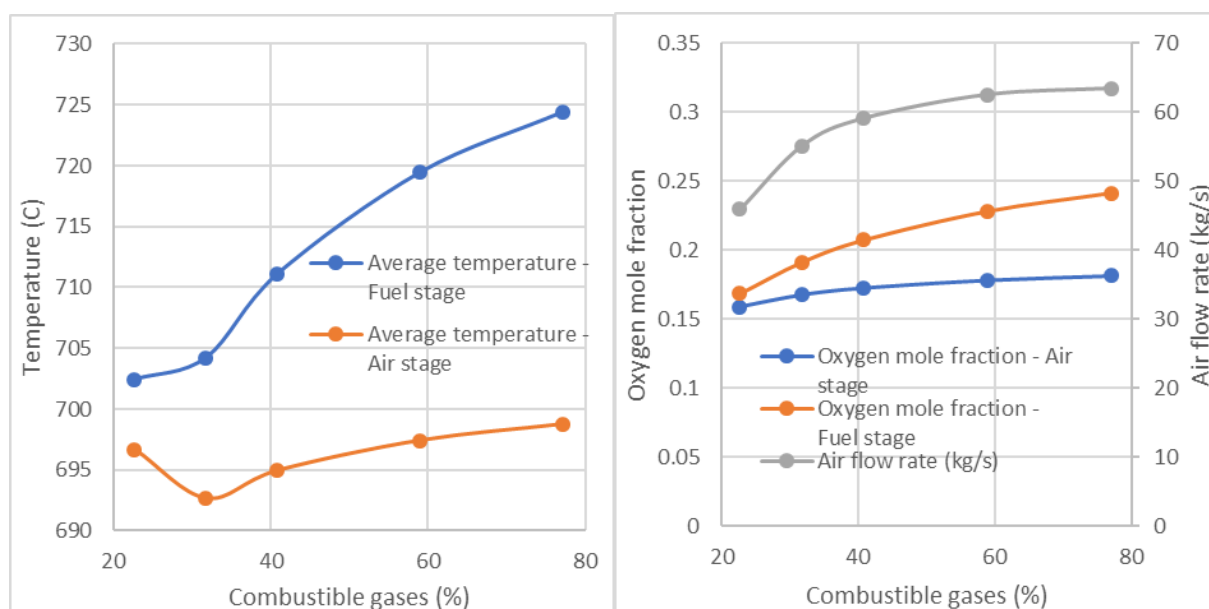


Figure 9: Influence of the amount of fuel gases in the reduction stage on the reactor temperature (left) as well as the oxygen mole fractions and outlet depleted air flowrate (right).

This trade-off can potentially be mitigated by including a pressure swing in the process, i.e., carrying out the reduction stage at a lower pressure than the oxidation stage. If the absolute pressure in the reduction stage is lowered, a higher oxygen mole fraction can be reached at a given equilibrium oxygen partial pressure. The simple standalone nature of the GSOP reactors can potentially facilitate the implementation of a moderate pressure swing, so this possibility will be explored in future work.

5 References

1. Wassie, S.A., et al., *Hydrogen production with integrated CO₂ capture in a novel gas switching reforming reactor: Proof-of-concept*. International Journal of Hydrogen Energy, 2017. **42**(21): p. 14367-14379.
2. Stull, D.R. and H. Prophet, *JANAF Thermochemical Tables*. 2nd Edition ed. 1971: National Bureau of Standards U.S.

3. Robie, R.A. and B.S. Hemingway, *Thermodynamic properties of minerals and related substances at 298.15 K and 1 bar (10⁵ pascals) pressure and at higher temperatures*, in *Bulletin*. 1995.
4. Abad, A., et al., *Kinetics of redox reactions of ilmenite for chemical-looping combustion*. *Chemical Engineering Science*, 2011. **66**(4): p. 689-702.
5. Xu, J. and G.F. Froment, *Methane steam reforming, methanation and water-gas shift: I. Intrinsic kinetics*. *AIChE Journal*, 1989. **35**(1): p. 88-96.
6. Rydén, M. and M. Arjmand, *Continuous hydrogen production via the steam–iron reaction by chemical looping in a circulating fluidized-bed reactor*. *International Journal of Hydrogen Energy*, 2012. **37**(6): p. 4843-4854.
7. Larring, Y., et al., *COMPOSITE: A Concept for High Efficiency Power Production with Integrated CO₂ Capture from Solid Fuels*. *Energy Procedia*, 2017. **114**: p. 539-550.
8. Cloete, S., et al., *Integration of a Gas Switching Combustion (GSC) system in integrated gasification combined cycles*. *International Journal of Greenhouse Gas Control*, 2015. **42**: p. 340-356.